Journal of Ginseng Research 46 (2022) 235–247

Contents lists available at ScienceDirect

Journal of Ginseng Research

journal homepage: https://www.sciencedirect.com/journal/journal-of-ginseng-research

Research Article

Ginsenoside Rg3 ameliorates myocardial glucose metabolism and insulin resistance via activating the AMPK signaling pathway

Jingyu Ni [a, b], Zhihao Liu [a], Miaomiao Jiang [c], Lan Li [a], Jie Deng [a], Xiaodan Wang [a], Jing Su [c], Yan Zhu [c], Feng He [b], Jingyuan Mao [a], Xiumei Gao [c, **, 1], Guanwei Fan [a, b, c, *, 1]

[a] National Clinical Research Center for Chinese Medicine Acupuncture and Moxibustion, First Teaching Hospital of Tianjin University of Traditional Chinese Medicine, Tianjin, China
[b] Hubei Key Laboratory of Economic Forest Germplasm Improvement and Resources Comprehensive Utilization, Huanggang Normal University, Huanggang, China
[c] Tianjin State Key Laboratory of Component-based Chinese Medicine, Tianjin University of Traditional Chinese Medicine, Tianjin, China

ARTICLE INFO

Article history:
Received 13 November 2020
Received in revised form
29 May 2021
Accepted 1 June 2021
Available online 5 June 2021

Keywords:
Glucose metabolism
Insulin resistance
Ginsenoside Rg3
AMPK
Heart failure

ABSTRACT

Background: Ginsenoside Rg3 is one of the main active ingredients in ginseng. Here, we aimed to confirm its protective effect on the heart function in transverse aortic coarctation (TAC)-induced heart failure mice and explore the potential molecular mechanisms involved.
Methods: The effects of ginsenoside Rg3 on heart and mitochondrial function were investigated by treating TAC-induced heart failure in mice. The mechanism of ginsenoside Rg3 for improving heart and mitochondrial function in mice with heart failure was predicted through integrative analysis of the proteome and plasma metabolome. Glucose uptake and myocardial insulin sensitivity were evaluated using micro-positron emission tomography. The effect of ginsenoside Rg3 on myocardial insulin sensitivity was clarified by combining *in vivo* animal experiments and *in vitro* cell experiments.
Results: Treatment of TAC-induced mouse models with ginsenoside Rg3 significantly improved heart function and protected mitochondrial structure and function. Fusion of metabolomics, proteomics, and targeted metabolomics data showed that Rg3 regulated the glycolysis process, and Rg3 not only regulated glucose uptake but also improve myocardial insulin resistance. The molecular mechanism of ginsenoside Rg3 regulation of glucose metabolism was determined by exploring the interaction pathways of AMPK, insulin resistance, and glucose metabolism. The effect of ginsenoside Rg3 on the promotion of glucose uptake in IR-H9c2 cells by AMPK activation was dependent on the insulin signaling pathway.
Conclusions: Ginsenoside Rg3 modulates glucose metabolism and significantly ameliorates insulin resistance through activation of the AMPK pathway.

1. Introduction

Heart failure is a serious stage of cardiovascular disease and the leading cause of death worldwide. It is a global public health problem that needs to be solved urgently. In the development of heart failure, not only ventricular remodeling but also metabolic remodeling are the causes of the decline of heart function [1–3]. Under normal circumstances, the heart produces energy mainly through the two pathways of free fatty acid and glucose oxidation. Approximately 60–70% of energy production in healthy hearts is derived from the β-oxidation of fatty acids, and approximately 20–30% is derived from the oxidation of glucose [4–6]. Changes in the two pathways of myocardial energy metabolism occur during heart failure. Among them, glucose metabolism is changed, which is mainly manifested by the weakening of the aerobic oxidation pathway of glucose by negative feedback regulation, enhanced glycolysis, and lactic acid accumulation. Therefore, regulating

* Corresponding author. Tianjin Key Laboratory of Translational Research of TCM Prescription and Syndrome, First Teaching Hospital of Tianjin University of Traditional Chinese Medicine, Tianjin, 300193, China.
** Corresponding author. Tianjin State Key Laboratory of Component-based Chinese Medicine Tianjin University of Traditional Chinese Medicine, Tianjin, 301617, China.
E-mail addresses: gaoxiumei@tjutcm.edu.cn (X. Gao), guanwei.fan@tjutcm.edu.cn (G. Fan).
[1] Present/permanent address: First Teaching Hospital of Tianjin University of Traditional Chinese Medicine, 88 Changling Road, Xiqing District, Tianjin, China.

https://doi.org/10.1016/j.jgr.2021.06.001

glucose metabolism to a normal state can delay the development of heart failure.

Glucose metabolism is affected by many signal transduction pathways, one of the most critical being the insulin signal pathway. The heart is also one of the main target organs for insulin action [7,8]. In heart failure, insulin sensitivity is impaired. When insulin resistance develops, myocardial glucose uptake and utilization are disturbed [9–11]. Epidemiological evidence [12,13] has confirmed the close relationship between heart failure and insulin resistance. On the one hand, insulin resistance is an independent risk factor for heart failure. On the other hand, insulin resistance is also more common in patients with heart failure, and the prognosis of patients with heart failure accompanied by insulin resistance is worse [14]. Although insulin resistance alone is not sufficient to cause heart failure, it can weaken the heart's compensatory ability under stress (ischemia, pressure load, or injury). Over time, the heart muscle is damaged, morphological and functional changes occur, and the occurrence and development of heart failure are accelerated [5,15–17]. Considering insulin resistance as a cause of heart failure will provide new strategies and targets for the treatment of heart failure.

As an energy receptor, AMPK can enhance glucose uptake, promote fatty acid oxidation, inhibit protein synthesis, and improve insulin resistance. It plays the role of a master switch in maintaining energy metabolic balance [18,19]. Moreover, there is a complex relationship between the AMPK and insulin signaling pathways at the molecular level. AMPK has become a target for the treatment of many metabolic diseases, including insulin resistance. AMPK is expected to become a new target for drugs to optimize glucose metabolism and improve myocardial insulin resistance [20,21].

Ginsenoside Rg3 is one of the main active ingredients isolated from ginseng, and it has a variety of pharmacological effects, including antioxidant, anti-inflammatory, anti-tumor, and anti-aging effects [22–26]. Our previous studies revealed that Rg3-loaded pluronic F127 micelles alleviate doxorubicin-induced oxidative stress by reversing mitochondrial dysfunction [25]. Moreover, Rg3-loaded PEG-b-PPS nanoparticles alleviate myocardial ischemia-reperfusion injury by interacting with the target protein, FoxO3a, inhibiting its downstream signaling pathways, including those for oxidative stress, inflammation, and fibrosis [26]. However, it is unclear whether the protective effect of ginsenoside Rg3 on cardiac function is due to regulating glucose metabolism and improving myocardial insulin resistance. Therefore, we investigated the potential mechanism of ginsenoside Rg3 for improving myocardial glucose metabolism and insulin resistance *in vivo* and *in vitro*.

2. Materials and methods

2.1. Transverse aortic coarctation (TAC) model preparation and drug administration

Male C57BL/6J mice were randomly divided into the following four groups: the (1) sham, (2) model, (3) Rg3-20 mg/kg, and (4) Rg3-10 mg/kg groups. The number of mice in each group was 25–30. The model of heart failure was induced via TAC, as described previously [27,28]. Four weeks after surgery, ginsenoside Rg3 (purity $\geq$ 98%; Shanghai Winherb Medical Technology Co., Ltd., Shanghai, China) suspended in normal saline was administered intraperitoneally once a day for four consecutive weeks (20 or 10 mg/kg/day). Mice in the sham and model group were administered normal saline in equal volume via intraperitoneal injection.

2.2. Echocardiographic assessment of left ventricular function

Left ventricular function was evaluated using the Vevo 2100 (VisualSonic, Canada) ultra-high resolution animal ultrasound imaging system, as described previously [28,29].

2.3. Hemodynamic examination

Hemodynamics analysis was carried out by using the bio-function experiment system MP100-CE (BIOPAC Systems, Inc., Santa Barbara, CA, USA). The left ventricular maximum upstroke velocity (+dp/dt max) and maximum decrease rate (-dp/dt min) were measured.

2.4. Histological analysis

Histologic sections of tissues were stained with hematoxylin/eosin and wheat germ agglutinin (WGA). For immunofluorescence analysis, sections were incubated with a mixture of mouse anti-goat COLIα2 or COLIIIα1 polyclonal antibody and rabbit anti-goat α-SMA polyclonal antibody (all dilutions at 1:250) at 4°C for 12 h. After washing with PBS, the sections were counterstained with a mixture of FITC-labeled goat anti-mouse IgG (1:30) and Cy3-labeled goat anti-rabbit IgG (1:40) at 37°C for 1 h. After washing with PBS, the sections were mounted with water-soluble anti-quenching 4′,6-diamidino-2-phenylindole (DAPI). The results were observed using a fluorescence microscope (Carl Zeiss, Axio Observer A1).

2.5. Real-time quantitative PCR

Real-time quantitative PCR was performed as previously described [30]. The primer sequences of ANP, BNP, α-SKA, and β-MHC were synthesized by Sangon Biotech Co., Ltd. (Shanghai, China) as follows: for ANP, TGGGACCCCTCCGATAGATC and TCGTGATAGATGAAGGCAGGAA; for BNP, GGAAGTCAACGGGAA-GAAGTTCACTG and CAATGTAACCGGCACCCACAATAAC; for β-MHC, TTGAGAATCCAAGGCTCAG C and CTTCTCAGACTTCCGCAGGA; for α-SKA, CAGCTCTGGCTCCCAGCAC C and AATGGCTGGCTT-TAATGCTTCA; and for GAPDH, CGGCCGCATCTTCTTGTG and CACC GACCTTCACCATTTTGT.

2.6. SDS-PAGE and western blotting

Western blot analysis was performed using the method previously described [29] with specific primary antibodies against IRS-1, Akt-1, AS160, PDK4, GLUT4, GLUT1, GAPDH (all from Proteintech, China), AMPK, p-AMPK (both from Thermo Scientific, USA), and total OXPHOS (from Abcam, UK).

2.7. Transmission electron microscopy (TEM)

For TEM, heart tissues were processed for ultrastructural analysis using the method previously described [26,30]. Pictures were taken from three random areas from three sections per mouse.

2.8. Mitochondrial respiration

The isolation of intact mitochondria from heart tissue was performed as previously described [31]. A BCA Protein Assay Kit (Thermo Fisher Scientific Inc, Massachusetts, USA) was used to quantify protein content in the mitochondria. The mitochondrial oxygen consumption rate was assessed with the Seahorse XF24 analyzer as previously described [32].

2.9. Mitochondrial inner membrane permeability

Langendorff perfusion of isolated mouse hearts was performed using the method previously described [33]. Tetramethylrhodamine ethyl ester (TMRE) and Mitotracker double staining were performed to detect mitochondrial inner membrane permeability in isolated myocardial cells.

2.10. Proteomics

Mass spectrometry analysis of iTRAQ was completed by Thermo Q-Exactive mass spectrometry, and the original mass spectrometry data generated were processed by Proteome Discoverer 1.4, a supporting commercial software of Thermo.

2.11. Metabolic profiling

Metabolic profiling based on NMR measurements was performed using the method previously described [34]. The obtained NMR integral data were normalized and Pareto scaled, then were imported into MetaboAnalyst 3.0 (www.metaboanalyst.ca) software for principal component analysis and orthogonal partial least squares discriminant analysis.

2.12. Quantitative analysis of energy metabolites in mouse heart tissue by LC-MS/MS

First, 1 mL of pre-cooled methanol/acetonitrile/water (2:2:1, v/v/v) was added to the sample. After the samples were vortex-mixed, they were sonicated for 30 min in an ice bath. The samples were then incubated at −20°C for 1 h to precipitate proteins, centrifuged at 14,000 rcf at 4°C for 20 min, and the supernatant was taken and dried in vacuo. For mass detection, 100 μL of acetonitrile-water solution (1:1, v/v) was added for reconstitution. After centrifugation at 1,4000 rcf at 4°C for 15 min, the supernatant was diluted twice and injected for analysis. The samples were separated using the Agilent 1290 Infinity LC ultra-high performance liquid chromatography system. The sample was placed in a 4°C auto-sampler, the column temperature was 45°C, the flow rate was 300 μL/min, and the injection volume was 4 μL. Samples were first used for evaluating the stability and repeatability of the system. The standard mixture of energy metabolites in the sample cohort was used to correct the chromatographic retention time. The 5500 QTRAP mass spectrometer (AB SCIEX) was used for mass spectrometry analysis in negative ion mode. The ion pair was detected in MRM mode. Multiquant software was used to extract the chromatographic peak area and retention time. Standards of energy metabolites were used to correct retention time, and metabolites were identified.

2.13. Glucose metabolism monitoring by 18-fluorodeoxyglucose small animal positron emission computed tomography

The mice were fed normally, and intraperitoneal injection of normal saline or 10–15 U/kg insulin was performed 30 min before the micro-positron emission tomography (PET) test. The oxygen flow was controlled at 400 mL/min and the tail vein bolus was injected with 50–70 μL of 18F-FDG 200–300 uci (7.4–11.1 MBq) for micro-PET dynamic imaging for 60 min under 1.5–1.8% isoflurane anesthesia. After image reconstruction, the myocardial region of interest was delineated to obtain the myocardial TAC, and the myocardial glucose standard uptake value (SUV) was calculated.

2.14. Cell viability assay

H9c2 cells were obtained from the cell bank of the Institute of Basic Medical Sciences, the Chinese Academy of Medical Sciences (Beijing, China). The MTT assay was used to detect the cell viability as previously described [29].

2.15. Glucose uptake in H9c2 cells using 2-NBDG as the fluorescence probe

H9c2 cardiomyocytes were seeded into 96-well plates with approximately 10^5 cells per well and were incubated for 24 h. Cells were treated with the corresponding reagents or drugs for 24 h. Cells were treated with 0 or 100 μmol/L insulin for 30 min, washed twice with KRB, then treated with 100 μmol/L 2-NBDG for 30 min at 37°C and washed twice with KRB. Changes in intracellular fluorescence intensity were measured using a fluorescence microplate reader (Ex/Em, 488/520 tim) to assess the uptake of 2-NBDG by H9c2 cardiomyocytes. Finally, the fluorescence intensity of cells in each well was corrected by MTT analysis.

2.16. Statistical analysis

The experimental processes and data analyses were carried out following randomization. The experimental data are expressed as the mean ± SD. GraphPad Prism 8.0 software was used for data analysis. A one-way ANOVA followed by an LSD post hoc test were used to test the differences between groups. A p value less than 0.05 was considered significant.

3. Results

3.1. Ginsenoside Rg3 reduced myocardial hypertrophy, delayed ventricular remodeling, and improved cardiac function

Ventricular remodeling is the main pathological basis for the occurrence and development of heart failure. Therefore, in this experiment, the effect of ginsenoside Rg3 on ventricular remodeling was observed.

To investigate the effect of ginsenoside Rg3 on TAC-induced HF, four weeks after TAC surgery, the mice were treated with either a low (10 mg/kg/day) or high dose (20 mg/kg/day) of Rg3. Ginsenoside Rg3 treatment groups exhibited significant improvement in myocardial hypertrophy, with decreased HW/TL, LV mass/TL ratios, systolic and diastolic left ventricular volume, and WGA (Fig. 1A–E). Lower expression of the ANP, BNP, β-MHC, and α-SKA genes provided further evidence of the protection of Rg3 in TAC-induced HF (Fig. 1F–I). Based on the histological assessment of heart tissues, we found reduction in cell size in Rg3-treated mice (Fig. 1J and K) and reduction in the content of type I and type III collagen in the heart (Fig. 1L–M).

Cardiac dysfunction is the main functional change of the heart during chronic heart failure. After four weeks of administration, the effects of ginsenoside Rg3 on cardiac functions were assessed by echocardiography. Compared with the model group, the amplitude of the left ventricular wall motion was stronger after treatment with ginsenoside Rg3. EF% and FS% were significantly increased after ginsenoside Rg3 treatment ($P < 0.01$ vs. Model, Fig. 1O–P). From the histological assessment of heart tissues, we found reduced inflammatory cell infiltration and diffuse edema in Rg3-treated mice (Fig. 2Q), indicating that ginsenoside Rg3 could improve cardiac function in mice with chronic heart failure induced by TAC. The maximum increase rate (+dp/dt max) and maximum decrease rate (-dp/dt max) in mice from the model group were decreased ($P < 0.01$ vs. Sham, $P < 0.01$ vs. Sham). The maximum

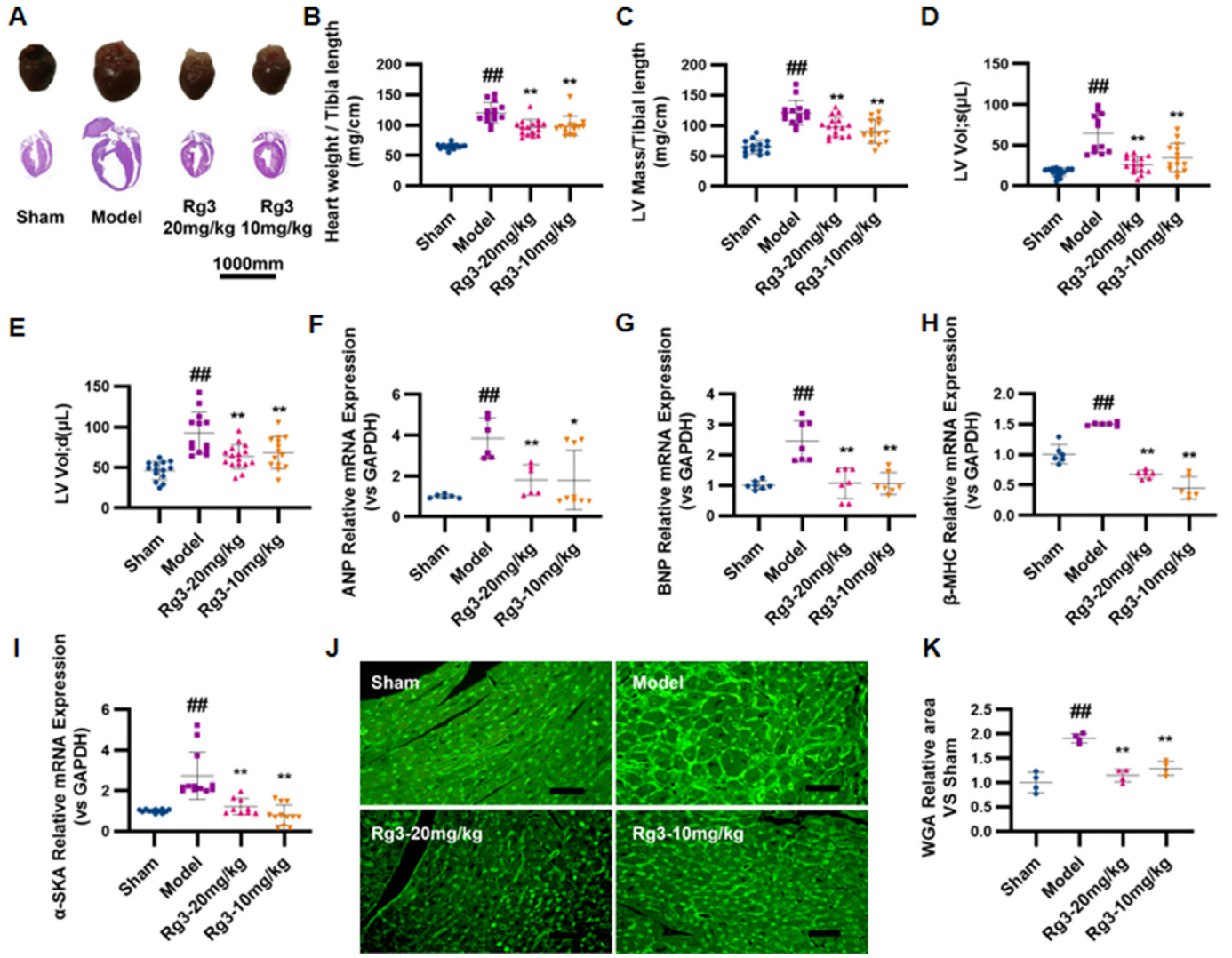

Fig. 1. Ginsenoside Rg3 reduced myocardial hypertrophy, delayed ventricular remodeling and improved cardiac function. (A) Representative images showing gross cardiac morphology of mice in each group. HE staining of longitudinal heart (n = 5). **(B)** Heart weights of C57BL/6 mice (n = 4). (C) Left ventricular mass of C57BL/6 mice (n = 15-16 each group). (D-E) Systolic left ventricular volume(n = 12-15 each group) (D), Diastolic left ventricular volume(n = 13-16 each group) (E). (F–I)Gene expression of the ANP(n = 6-9 each group) (F), BNP(n = 7 each group) (G), β-MHC(n = 6 each group) (H) and α-SKA(n = 9-12 each group) (I). (J-K)WGA staining(n = 3 each group) (J), WGA staining quantification chart(n = 4 each group) (K). (L-M)For immunofluorescence analysis, sections were incubated with a mixture of mouse anti-goat COLIα2(n = 6 each group) (L) or COLIIIα1(n = 6 each group) (M) polyclonal antibody and rabbit anti-goat α-Skactin polyclonal antibody(n = 5-8 each group). (N)Representative M-mode echocardiograms of mice in each group. (O–P)Left ventricular ejection fraction(EF%, n = 12-15 each group) and fractional shortening(FS%, n = 13-16 each group) were assessed by serial echocardiography. (Q)H&E staining of transverse sections(n = 3 each group). Scale bars, 50 μm. (R)Left ventricular pressure-volume loops(n = 3 each group). (S-T)Effect on the maximum rate of left ventricle rise and the maximum rate of left ventricle fall(n = 3-4 each group). #P < 0.05 vs sham, ##P < 0.01 vs sham; *P < 0.05 vs model, **P < 0.01 vs model.

decrease rate was not significantly improved after administration of ginsenoside Rg3. However, the administration of ginsenoside Rg3 significantly improved the maximum increase rate ($P < 0.05$, vs. model, Fig. 1R–T).

These results confirmed that ginsenoside Rg3 improved the cardiac function in TAC-induced chronic heart failure mice.

3.2. Ginsenoside Rg3 improves mitochondrial ultrastructure and function

During the development of heart failure, the failed heart often experiences changes in energy metabolism and substrate utilization at the mitochondrial level. Therefore, mitochondrial structure and function were evaluated in this study.

The ultrastructure of mitochondria was observed through TEM. Compared with the Sham group, myocardial mitochondria in the TAC model group showed disordered arrangement, obvious edema, and ablation of the mitochondrial crest. After treatment with ginsenoside Rg3, the mitochondria of the myocardium were neatly arranged, mitochondrial edema was reduced, and the mitochondrial crest was relatively clear and complete (Fig. 2A). To investigate whether ginsenoside Rg3 treatment resulted in changes in mitochondrial function, the cells were loaded with TMRE to indicate mitochondrial inner membrane permeability. Compared with the Sham group, TMRE fluorescence intensities were obviously weakened in myocardial cells in the model group, whereas ginsenoside Rg3 treatment resulted in enhanced fluorescence intensity (Fig. 2B). The potential of ginsenoside Rg3 for enhancing

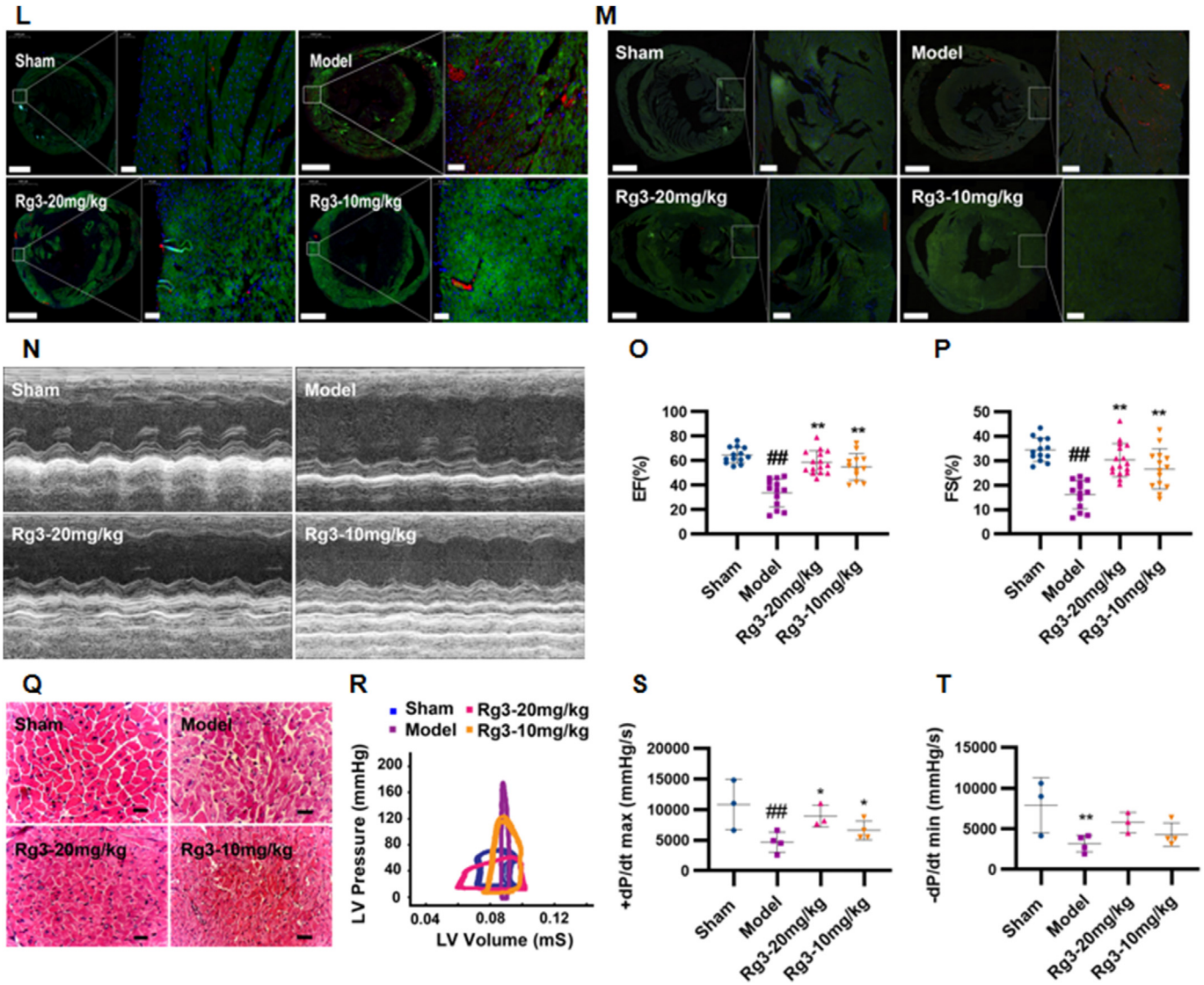

Fig. 1. (*continued*).

mitochondrial function in cardiac hypertrophy was assessed by ATP production, spare respiratory capacity, and maximal mitochondrial respiration rates. Hypertrophic myocardial cells showed a significant decline in ATP production, spare respiratory capacity, and maximal mitochondrial respiration rates in comparison with the Sham group (Fig. 2C–F). Ginsenoside Rg3 treatment resulted in increased ATP production ($P < 0.01$, vs. model), improved spare respiratory capacity ($P < 0.05$, vs. model), and enhanced maximal mitochondrial respiration rates ($P < 0.01$, vs. model).

Furthermore, to confirm the effect of ginsenoside Rg3 on mitochondrial function, we detected the protein content of transport chain complexes (ETC) in isolated mitochondria from the heart tissue. As shown in Fig. 2G–L, the protein content of complexes I, II, III, and IV showed no significant changes in the TAC and Rg3 treatment groups.

These results confirmed that ginsenoside Rg3 improved the mitochondrial ultrastructure and function in mice with chronic heart failure induced by TAC.

3.3. Fusion of proteomics and metabolomics data showed that ginsenoside Rg3 had a moderating effect on glycolysis/gluconeogenesis

Differential proteins were screened using Maxquant's Significance A to calculate the p value after calculating the corresponding ratio. A fold change of 1.5 times and p value < 0.05 were considered to indicate significant differences. Heatmap analysis (Fig. 3A and B) showed that ginsenoside Rg3-20 mg/kg had a significant effect on 16 abnormally changed proteins and ginsenoside Rg3-10 mg/kg had a significant effect on 25 abnormally changed proteins in the heart failure model. The metabolite profiles of mouse plasma were collected using ^{1}H-NMR technology. When the screening condition was VIP > 1, 275, 221, and 278 variables were extracted from the three comparisons, and 59 variables related to heart failure, which were regulated by ginsenoside Rg3, were further screened by Venn analysis. Based on the structural information provided by each variable, 10 metabolites were identified (Fig. 3C) as key metabolic markers related to heart failure regulated by ginsenoside Rg3.

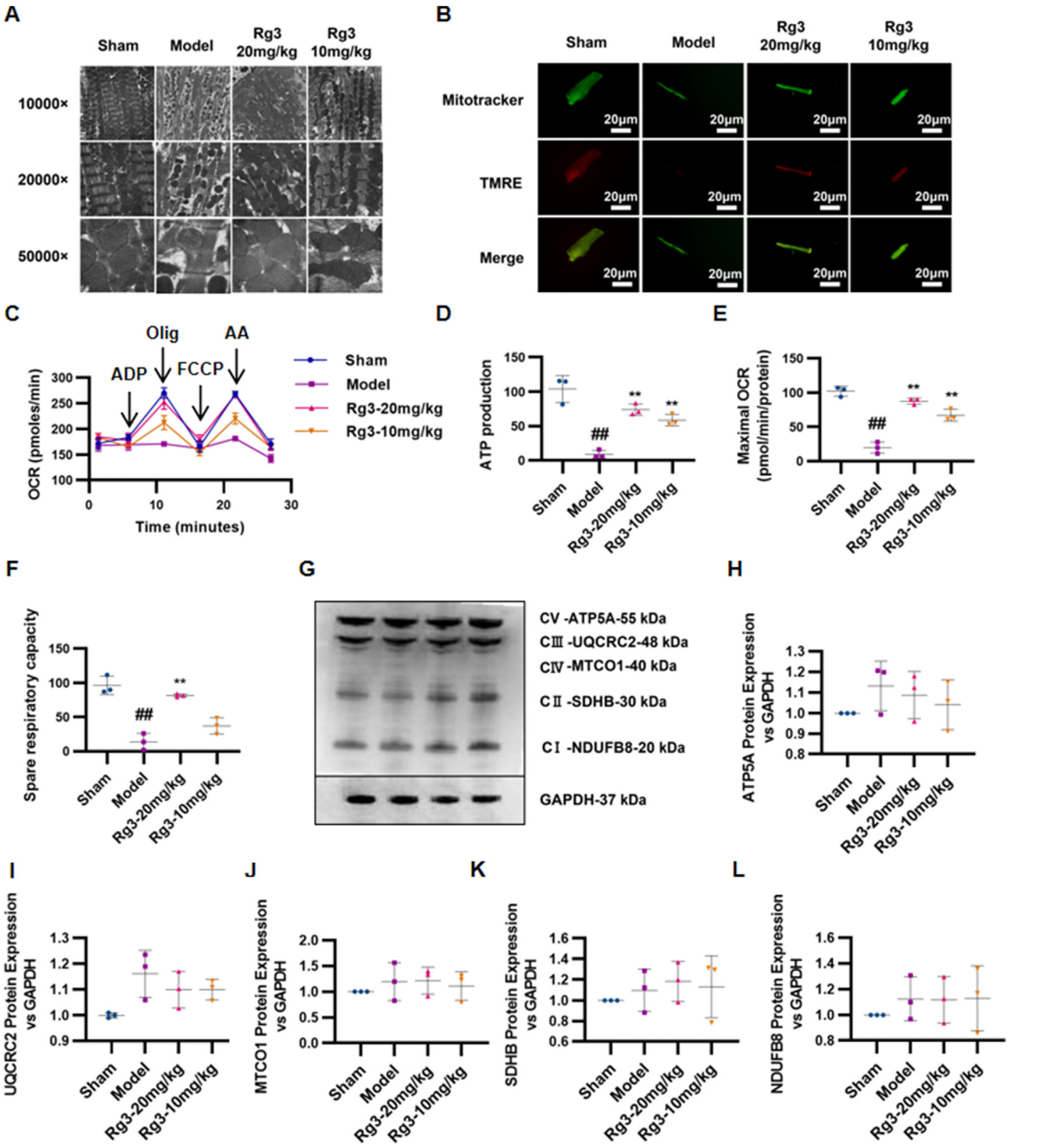

Fig. 2. Ginsenoside Rg3 improved mitochondrial ultrastructure and function in mice with chronic heart failure induced by TAC. (A)Ultrastructural analysis of mitochondrial integrity by transmission electron microscopy(n = 3 each group). (B)Tetramethylrhodamine ethyl ester (TMRE) and Mitotracker double staining were performed to detect mitochondrial inner membrane permeability in isolated myocardial cells(n = 3-4 each group). (C–F)Oxygen consumption rate (OCR) in mitochondria isolated from the hearts of various groups was measured with a Seahorse metabolic analyzer, ATP production, spare respiratory capacity and maximal mitochondrial respiration rates were then quantified. (G)Representative western immunoblots for oxidative phosphorylation (OXPHOS) complexes(n = 3 each group). (H-L)Bar graph showing corresponding quantitative data for western blotting(n = 3 each group). #P < 0.05 vs sham, ##P < 0.01 vs sham; *P < 0.05 vs model, **P < 0.01 vs model.

Next, we conducted a joint analysis of proteomics and metabolomics data, and the screening method was based on the previous literature [35]. Proteins with a fold change $\geq$ 1.5 and a p value < 0.05 were significantly differently expressed proteins. Metabolites with a fold change $\geq$ 1.5 and a p value < 0.1 were significantly differentially expressed metabolites. A total of 118 differential proteins and 18 differential metabolites were screened. Detailed analysis of the enrichment pathway showed that three

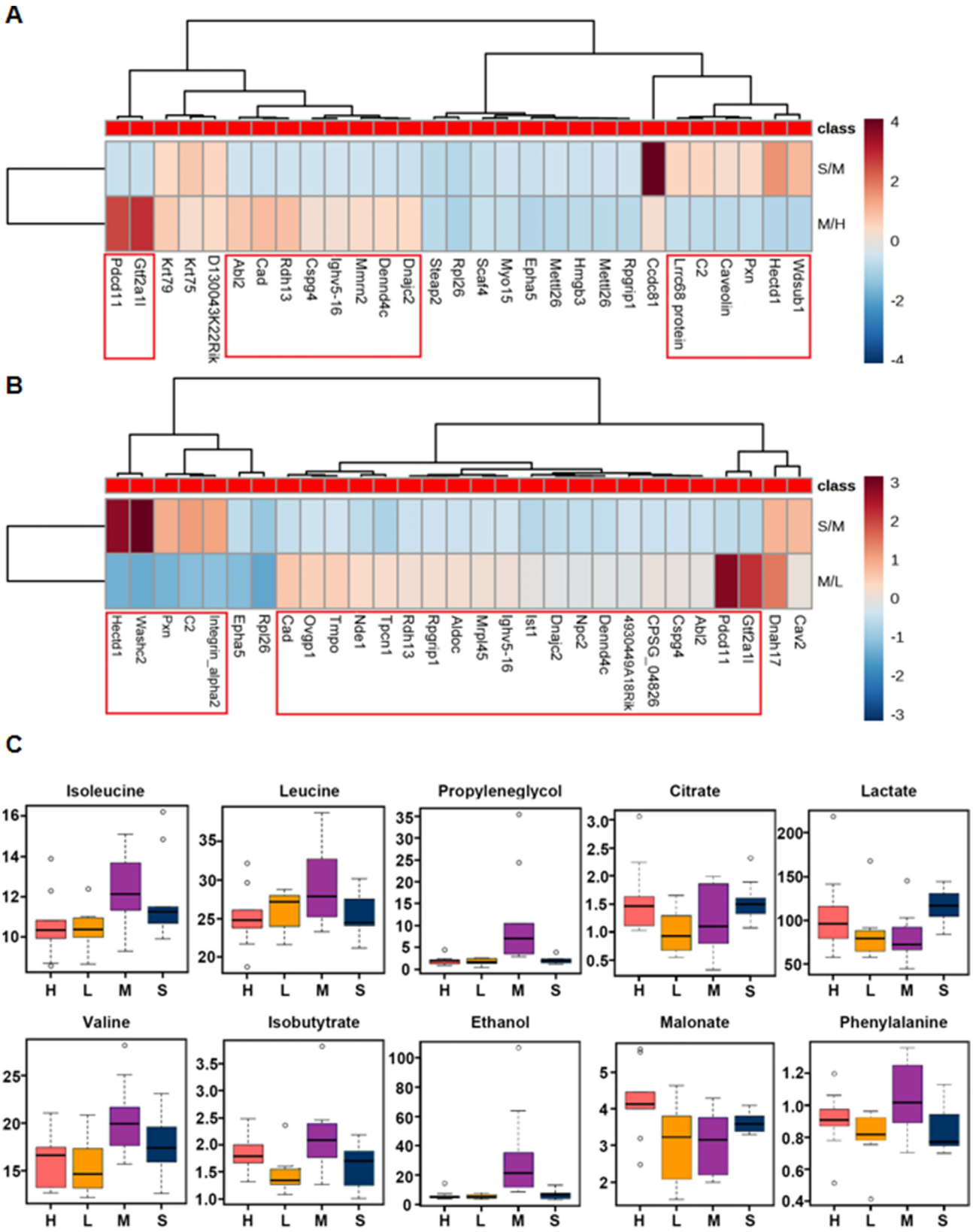

Fig. 3. Proteomics and metabolomics results. (A-B)Proteomics results of mice heart tissue in each group(n = 3 each group). (C)Metabolomics results of plasma in each group(n = 6-8 each group).

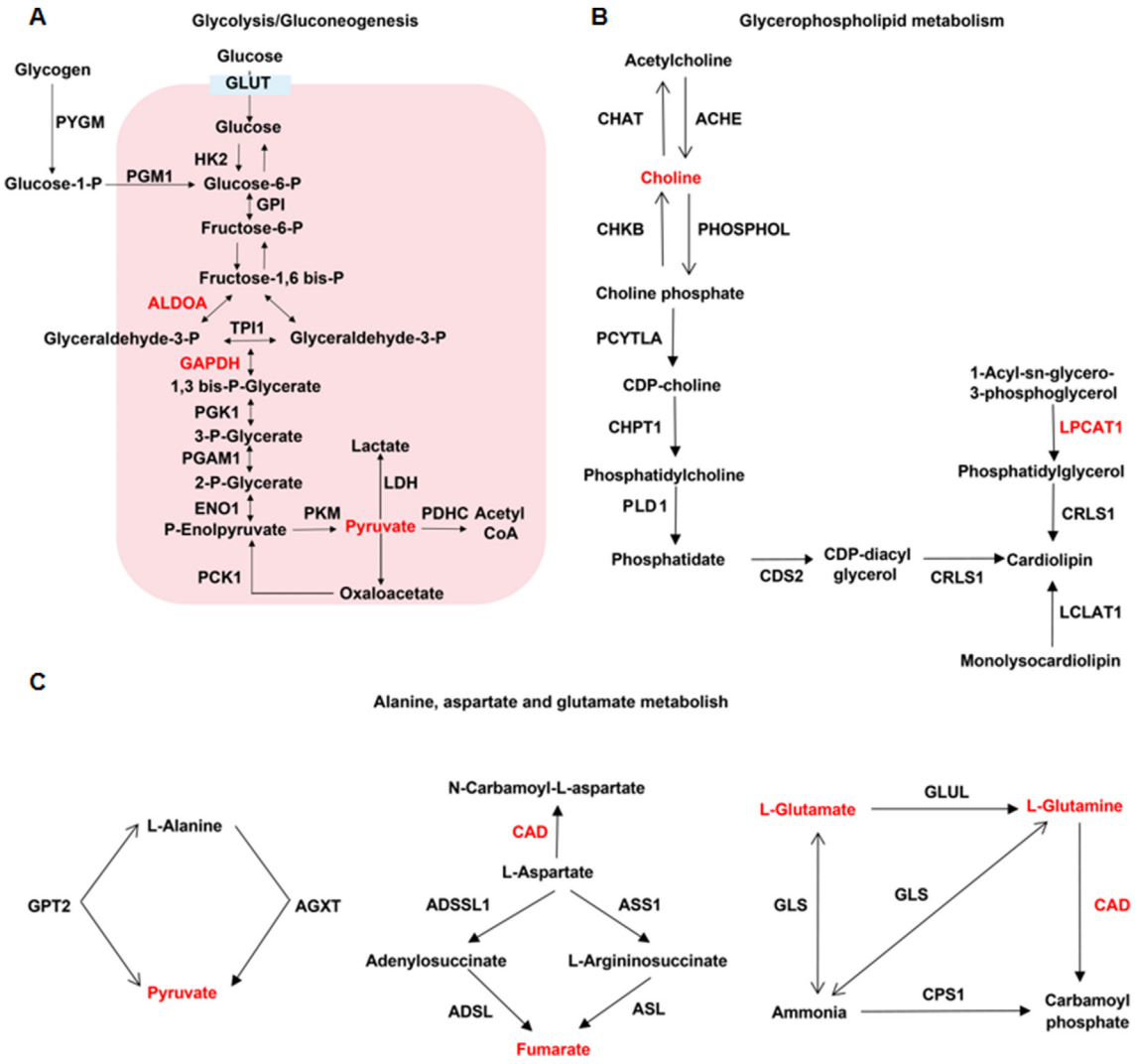

Fig. 4. Fusion of proteomics and metabolomics data showed that ginsenoside Rg3 had a moderating effect on glycolysis/gluconeogenesis. (A)Glycolysis/gluconeogenesis. **(B)** Glycerophospholipid metabolism. **(C)** Alanine, aspartate and glutamate metabolism.

pathways, glycolysis/gluconeogenesis, glycerophospholipid metabolism, and alanine/aspartate/glutamate metabolism, were involved in both differential proteins and differential metabolites (Fig. 4A–C).

3.4. Quantitative analysis of energy metabolites showed that ginsenoside Rg3 exerted significant homeostatic effects on multiple metabolites during glycolysis and the tricarboxylic acid cycle

Based on the results of the joint analysis of proteomics and metabolomics, we next examined the content of 17 important metabolites in the glycolytic pathway and the tricarboxylic acid cycle by LC-MS/MS. Using a detection process shown in Fig. 5A, results were quantified according to the metabolic pathways. The results showed that ginsenoside Rg3 exerted a significant homeostatic effect on phosphoenolpyruvate, pyruvate, acetyl CoA, aconitic acid, isocitrate, succinic acid, fumaric acid, and oxaloacetic acid (Fig. 5B).

3.5. Ginsenoside Rg3 regulated glucose uptake and myocardial insulin sensitivity

The above results revealed that the altered glucose metabolism in mice with heart failure can be effectively restored by ginsenoside Rg3. Therefore, protein expression levels of glucose transporter 4 (GLUT4) were detected to further investigate the effect of ginsenoside Rg3 on substrate utilization changes. As shown in Fig. 5C–E, the myocardial GLUT4 level was significantly increased in the Model group compared with that in the Sham group. Both high (20 mg/kg) and low (10 mg/kg) doses of ginsenoside Rg3 normalized glucose utilization. Changes in myocardial glucose metabolism in mice were monitored using 18-fluorodeoxyglucose (18-FDG) micro-PET. In the basal state, compared with the Sham group, the myocardial SUV in the Model group was significantly increased ($P < 0.05$). In contrast, treatment with ginsenoside Rg3 (20 mg/kg) significantly reduced myocardial glucose metabolism compared with that in the Model group ($P < 0.05$). These results showed that ginsenoside Rg3 had a significant regulatory effect on myocardial glucose metabolism in chronic heart failure induced by TAC (Fig. 5F and G). However, under insulin stimulation, myocardial glucose

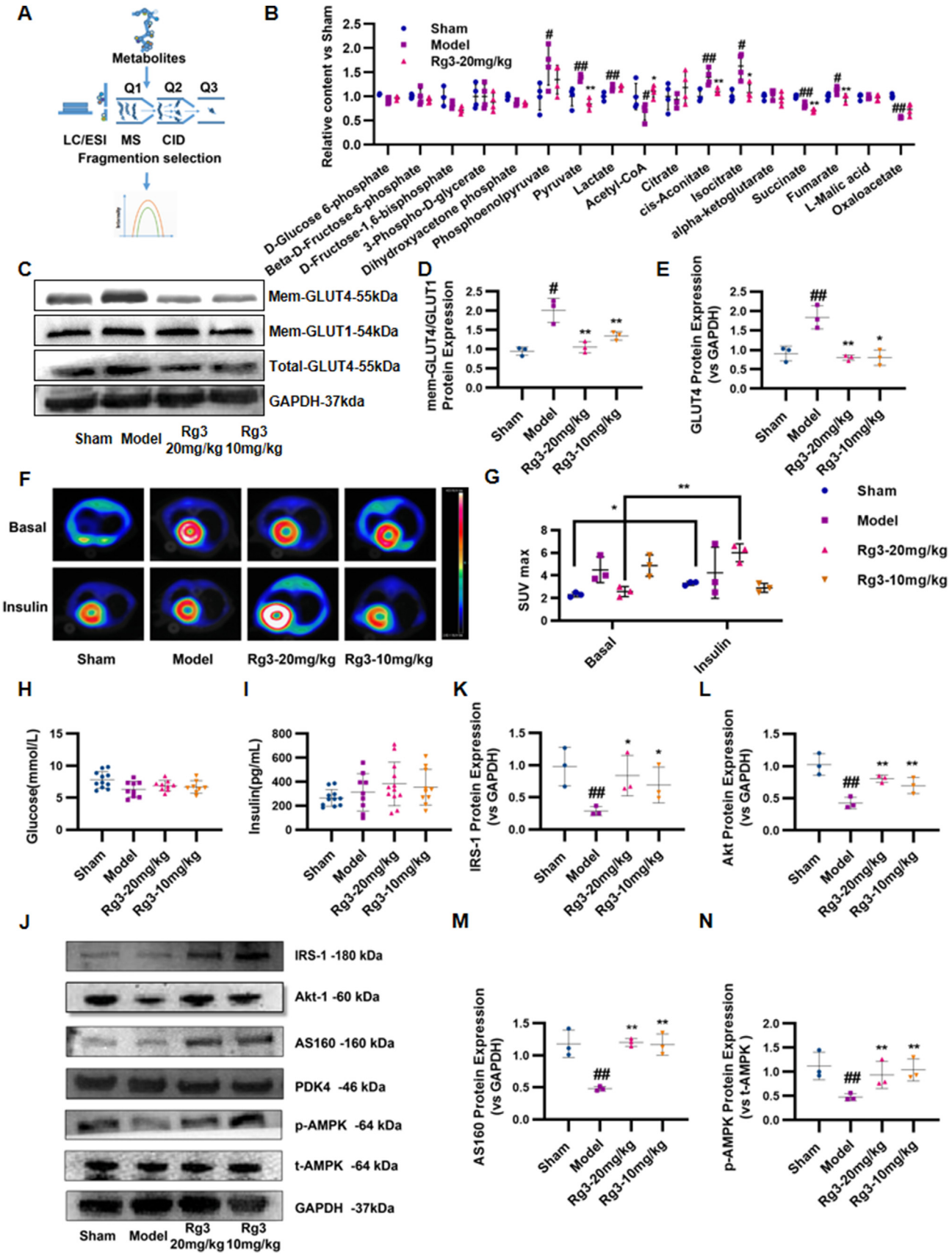

Fig. 5. Ginsenoside Rg3 regulated glucose uptake and myocardial insulin sensitivity in mice with heart failure. (A-B)Quantitative analysis of energy metabolites in mouse heart tissue by LC-MS/MS (n = 4 each group). (C)Representative Western immunoblots for GLUT4 and GLUT1 (n = 3 each group). (D-E)Bar graph showing corresponding quantitative data for western blotting (n = 3 each group). (F-G)Glucose uptake in mice were observed using 18-fluorodeoxyglucose positron emission tomography. The myocardial glucose standard

metabolism in the Sham group significantly increased. Compared with the Sham group, myocardial SUV in the Model group did not increase significantly after insulin stimulation, suggesting that the mice in the Model group had myocardial insulin resistance. Ginsenoside Rg3 (20 mg/kg) significantly increased the myocardial glucose metabolism after insulin stimulation ($P < 0.05$), suggesting that ginsenoside Rg3 significantly improved the myocardial insulin resistance in chronic heart failure induced by TAC (Fig. 5F and G). At the same time, systemic insulin sensitivity was also measured, but there was no significant change in serum glucose and insulin levels between groups (Fig. 5H and I).

3.6. Ginsenoside Rg3 had a regulatory effect on protein levels in the myocardial insulin signaling pathway and the phosphorylation of AMPK protein

Since systemic insulin sensitivity did not change significantly, we focused on myocardial insulin resistance. When myocardial insulin resistance occurs, it blocks the IRS-PI3K-Akt signaling pathway, which is associated with GLUT4 transport and translocation, thereby affecting myocardial substrate utilization and energy metabolism. Therefore, expression of the IRS-PI3K-Akt signaling pathway-related proteins was detected. As shown in Fig. 5, the expression of IRS1, Akt, and AS160 proteins in the myocardial IRS-PI3K-Akt signaling pathway in the model group was inhibited compared with that in the Sham group, leading to a disorder of myocardial glucose metabolism. Treatment with ginsenoside Rg3 (20 mg/kg) increased the expression of the IRS-PI3K-Akt signaling pathway-related proteins (Fig. 5J–N).

As an energy regulator, AMPK has received increasing attention regarding the regulation of intracellular energy balance. The AMPK signaling pathway plays an important regulatory role in glucose, fatty acid, and protein metabolism. In the present study, the protein level of phosphorylated AMPK was detected. Compared with the Sham group, the phosphorylated AMPK protein expression in the model group was reduced, which was restored by treatment with ginsenoside Rg3 at either high (20 mg/kg) or low (10 mg/kg) doses, suggesting that AMPK might be a potential target for ginsenoside Rg3 to regulate glucose metabolism.

3.7. The effect of ginsenoside Rg3 on the promotion of glucose uptake in IR-H9c2 cells by AMPK activation was dependent on the insulin signaling pathway

We established an IR-H9c2 cardiomyocyte model with high concentration insulin treatment to investigate the effect of ginsenoside Rg3 on glucose uptake and AMPK activity. MTT results showed that there was no significant difference in cell proliferation between treatment with 0.1, 1, or 10 μmol/L ginsenoside Rg3 and that in the control group (0 μg/mL) ($P > 0.05$). However, when the concentration of ginsenoside Rg3 reached 100 μmol/L, it had a significant inhibitory effect on the proliferation of H9c2 cardiomyocytes ($P < 0.05$, Fig. 6A). Therefore, 10 μmol/L was selected as the treatment concentration of ginsenoside Rg3 in the subsequent experiments. In normal H9c2 cells, there was no significant difference in the total AMPK protein expression in each group. However, ginsenoside Rg3 substantially increased the AMPK phosphorylation at Thr172. Compound C, a selective inhibitor of AMPK, significantly reduced the phosphorylation level of AMPK at Thr172 in H9c2 cardiomyocytes stimulated by ginsenoside Rg3 (Fig. 6B and C). In IR-H9c2 cells, the phosphorylation of AMPK at Thr172 was decreased significantly in the IR group compared with that in the control group ($P < 0.01$), whereas ginsenoside Rg3 significantly increased the phosphorylation of AMPK at Thr172 compared with that of the IR group ($P < 0.01$). Compound C significantly reduced the phosphorylation level of AMPK at the Thr172 of ginsenoside Rg3-stimulated IR-H9c2 cardiomyocytes (Fig. 6D and E). Next, the effect of ginsenoside Rg3 on glucose uptake in IR-H9c2 cardiomyocytes was evaluated using a fluorescent probe for glucose uptake 2-NBDG. Compared with that in the control group, the sensitivity to insulin in the IR group decreased, and insulin-stimulated glucose uptake was significantly reduced ($P < 0.05$), suggesting that there was insulin resistance in H9c2 cells in the IR group. Compared with the IR group, ginsenoside Rg3 significantly increased insulin-stimulated glucose uptake ($P < 0.05$). To confirm whether AMPK is involved in glucose uptake stimulated by ginsenoside Rg3 in IR-H9c2 cardiomyocytes, Compound C was used to pretreat IR-H9c2 cardiomyocytes and glucose uptake was measured. Compound C significantly reduced ginsenoside Rg3-stimulated glucose uptake in IR-H9c2 cardiomyocytes. The results suggested that ginsenoside Rg3 can promote the glucose uptake of IR-H9c2 cardiomyocytes, and this effect is related to the activation of AMPK (Fig. 6F). Based on our previous experiments, the IRS1 gene was silenced in cardiomyocytes, and changes in glucose uptake levels were observed. Moreover, the activator 5-Aminoimidazole-4-carboxamide1-β-D-ribofuranoside (AICAR) was used to investigate whether the effect of ginsenoside Rg3 on promoting glucose uptake in IR-H9c2 cells by activating AMPK is dependent on the insulin signaling pathway. The results showed that the effect of ginsenoside Rg3 on the promotion of glucose uptake in IR-H9c2 cells by AMPK activation was dependent on the insulin signaling pathway (Fig. 6G).

4. Discussion

The substrates of cardiac energy metabolism are mainly fatty acids and glucose, and the rate of heart work is closely related to the metabolic rate of energy substrates. Although glucose is only a secondary substrate for cardiac metabolism, it produces more energy than fatty acid metabolism when the same unit of oxygen is consumed. In the early stages of heart failure, myocardial metabolism begins to shift to glucose metabolism. In this way, the myocardium can complete the tricarboxylic acid cycle with little oxygen to produce more energy. However, as the disease progresses, compensatory glycolysis increases, and the balance between glycolysis and glucose oxidation is severely disturbed. The increased glycolysis not only does not compensate for the lack of energy, but also does not match the rate of oxidation of pyruvate and lactic acid, resulting in a large accumulation of hydrogen ions and calcium ions in the cytoplasm, leading to further damage to heart function. Therefore, inducing and improving the glucose oxidation pathway and reducing increased compensatory glycolysis is an important strategy for the treatment of heart failure [36–38].

In this study, since proteomics and metabolomics analysis revealed that ginsenoside Rg3 could regulate the glycolysis and gluconeogenesis pathways, we performed multiple reaction monitoring (MRM)-based quantitative analysis of the energy metabolites in mouse heart tissue. The test covered 17 important metabolites in the glycolysis pathway and the tricarboxylic acid cycle. The results showed that ginsenoside Rg3 had a significant

uptake value (SUV) was calculated (n = 3 each group). (H–I)Serum glucose and insulin was detected by ELISA kit (n = 6 each group). (J)Representative western immunoblots for IRS-1, Akt-1, AS160, PDK4, AMPK and GAPDH(n = 3 each group). (K–N)Bar graph showing corresponding quantitative data for Western blotting(n = 3 each group). #P < 0.05 vs sham, ##P < 0.01 vs sham; *P < 0.05 vs model, **P < 0.01 vs model.

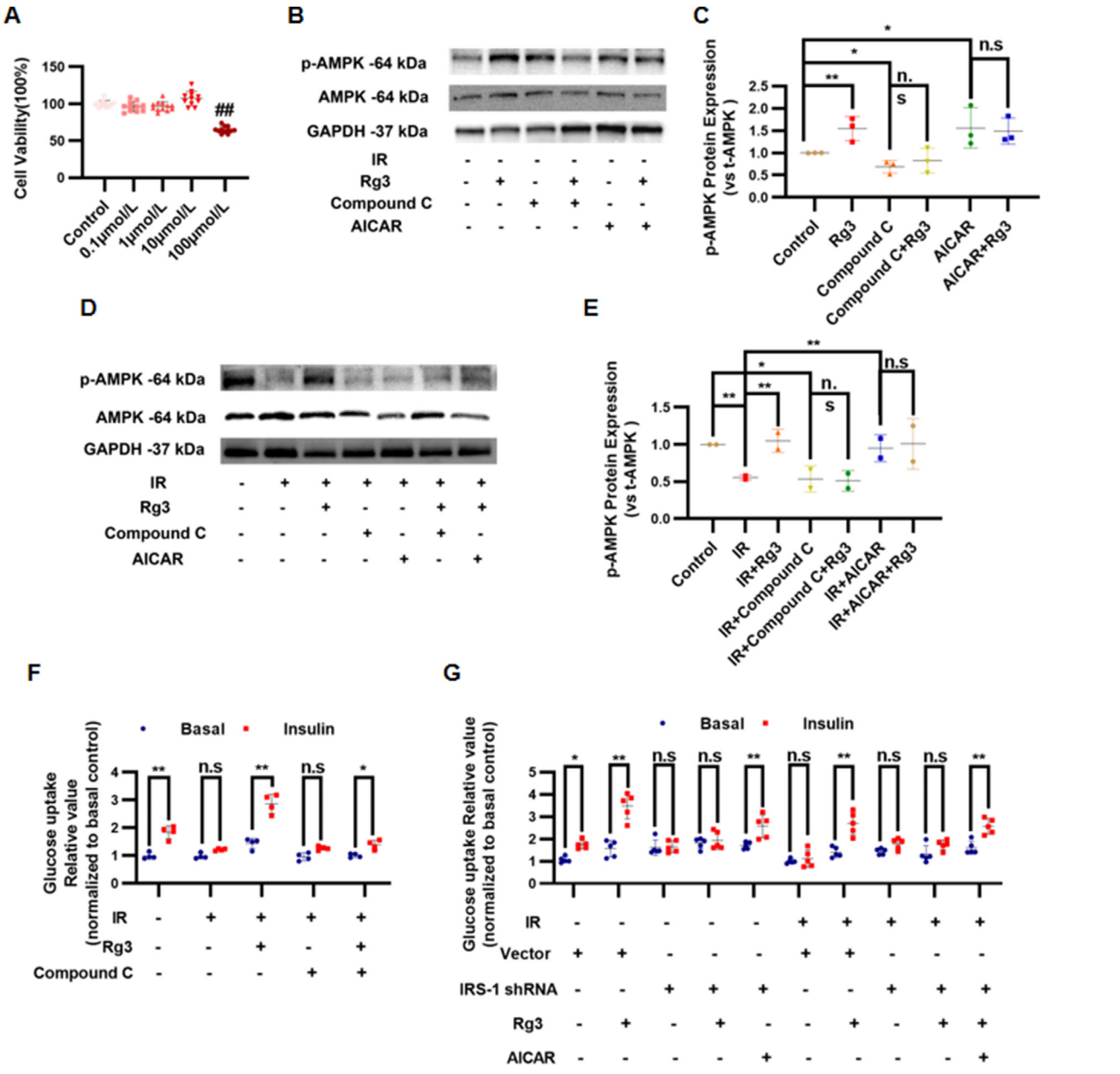

Fig. 6. The effect of ginsenoside Rg3 on the promotion of glucose uptake in IR-H9c2 cells by AMPK activation was dependent on the insulin signaling pathway. (A)The cell viability was detected by MTT assay(n = 10-12 each group). (B)Representative Western immunoblots for p-AMPK and t-AMPK in normal H9c2 cells(n = 3 each group). (C)Bar graph showing corresponding quantitative data for Western blotting(n = 3 each group). (D)Representative western immunoblots for p-AMPK and t-AMPK in IR-H9c2 cardiomyocytes(n = 3 each group). (E)Bar graph showing corresponding quantitative data for western blotting(n = 3 each group). (F-G)Glucose uptake in IR-H9c2 cardiomyocytes was evaluated using 2-NBDG fluorescent probes(n = 3 each group).

recuperative effect on phosphoenolpyruvate, pyruvate, and acetyl CoA. Aconitic acid, isocitric acid, succinic acid, fumaric acid, and oxaloacetic acid were significantly regulated during the tricarboxylic acid cycle. These results indicated that compensatory glycolysis in the myocardium of heart failure mice increased, which was reduced by ginsenoside Rg3, thereby achieving a balance between glycolysis and oxidation.

In this study, the proteomics and metabolomics results suggested that ginsenoside Rg3 might have a regulatory effect on alanine/aspartate/glutamate metabolism and glycerophospholipid metabolism, a finding worthy of in-depth study in future. The mechanistic analysis in this study was performed only at the cellular level, and there were certain limitations. Because the cell environment is relatively simple, the mechanism should be further explored at the organ level in subsequent studies.

Insulin resistance refers to the ability of insulin to promote glucose uptake, with utilization by target organs/tissues being reduced, resulting in a series of pathophysiological changes. The link between insulin resistance and heart failure has been proposed for more than a century. Epidemiological evidence suggests that insulin resistance and heart failure go far beyond a simple correlation. A Swedish study in 2005 of 1,187 male patients who had not previously experienced heart failure confirmed that insulin resistance precedes heart failure and is not subsequent to it. They also found that insulin resistance is predictive of subsequent heart failure and is independent of all established risk factors, including

diabetes [12]. A 2013 USA clinical study [13] more directly explored the relationship between insulin resistance and heart failure. The study included 12,606 subjects without heart failure and found that insulin resistance occurs before heart failure and is independent of other risk factors, including diabetes. This epidemiological evidence confirmed the close relationship between heart failure and insulin resistance, suggesting that insulin resistance is an independent risk factor for the development of heart failure. However, patients with heart failure also more commonly have insulin resistance, and patients with heart failure associated with insulin resistance have a worse prognosis [14]. The occurrence of insulin resistance is time phase- and tissue-specific. The heart is one of the main target organs for insulin action [7]. Clinical studies found that after scanning the myocardium of patients with heart failure with PET, the uptake of FDG in the myocardium under insulin stimulation was significantly reduced, indicating the presence of myocardial insulin resistance [8]. Therefore, patients with heart failure not only have systemic insulin resistance, but also often have myocardial insulin resistance. However, because the myocardium only accounts for 0.5% of the body weight, it has little effect on the overall blood glucose level, and myocardial insulin sensitivity has not attracted much attention. Increasing evidence shows that myocardial insulin resistance is directly related to the occurrence and development of cardiovascular disease.

In this study, micro-PET was used to observe changes in glucose uptake and metabolism in the myocardium of mice under insulin stimulation. The results showed that the Model group had myocardial insulin resistance, and ginsenoside Rg3 could significantly improve the myocardial insulin resistance of chronic heart failure induced by TAC.

AMPK, an energy sensor, regulates multiple physiological processes in the cardiovascular system and could be a potential therapeutic target. Upregulation of AMPK can affect multiple signaling pathways. For example, AMPK can inhibit the mTOR signaling pathway to inhibit protein synthesis, activate ULK1 to promote autophagy, and activate ATGL to promote fatty acid metabolism. In this study, we mainly investigated the effect of AMPK on the insulin signaling pathway and glucose metabolism, which has certain limitations. The effects of AMPK on other metabolic pathways are also worthy of investigation in future studies.

5. Conclusion

Ginsenoside Rg3 modulates glucose metabolism and significantly ameliorates insulin resistance through activation of the AMPK pathway.

Ethics approval and consent to participate

The experimental procedures conformed to the Directive 2010/63/EU of the European Parliament, and all animals were handled according to the guidelines of the TCM Animal Research Committee (TCM-LAEC2014005) of Tianjin University of Traditional Chinese Medicine.

Availability of data and materials

All data are provided and available in this manuscript.

Author contributions

Guanwei Fan, Xiumei Gao, Jingyuan Mao and Jingyu Ni designed experiments; Jingyu Ni, Zhihao Liu, Jie Deng and Xiaodan Wang carried out experiments; Miaomiao Jiang, Lan Li, Yan Zhu and Feng He analyzed experimental results. Jingyu Ni wrote the manuscript. All authors reviewed and edited this manuscript.

Declaration of competing interest

The authors declare that they have no competing interests. No conflict of interest exits in the submission of this manuscript, and manuscript is approved by all authors for publication. All authors declare no other relationships or activities that could appear to have influenced the submitted work.

Acknowledgements

This work was supported by grants from the National Key Subject of Drug Innovation (No.2019ZX09201005-007), Tianjin Outstanding Youth Science Foundation (No.17JCJQJC46200), the National Natural Science Foundation of China (No.81774050), the Natural Science Foundation of Tianjin (17JCYBJC29000).

References

[1] van Bilsen M, Smeets PJ, Gilde AJ, van der Vusse GJ. Metabolic remodelling of the failing heart: the cardiac burn-out syndrome? Cardiovasc Res 2004;61:218–26.
[2] Ritchie RH, Delbridge LM. Cardiac hypertrophy, substrate utilization and metabolic remodelling: cause or effect? Clin Exp Pharmacol Physiol 2006;33:159–66.
[3] Bertero E, Maack C. Metabolic remodelling in heart failure. Nat Rev Cardiol 2018;15:457–70.
[4] Doenst T, Nguyen TD, Abel ED. Cardiac metabolism in heart failure: implications beyond ATP production. Circ Res 2013;113:709–24.
[5] Doehner W, Frenneaux M, Anker SD. Metabolic impairment in heart failure: the myocardial and systemic perspective. J Am Coll Cardiol 2014;64:1388–400.
[6] Lopaschuk GD, Ussher JR. Evolving concepts of myocardial energy metabolism: more than just fats and carbohydrates. Circ Res 2016;119:1173–6.
[7] Rask-Madsen C, Kahn CR. Tissue-specific insulin signaling, metabolic syndrome, and cardiovascular disease. Arterioscler Thromb Vasc Biol 2012;32:2052–9.
[8] Heck PM, Dutka DP. Insulin resistance and heart failure. Curr Heart Fail Rep 2009;6:89–94.
[9] Guo CA, Guo S. Insulin receptor substrate signaling controls cardiac energy metabolism and heart failure. J Endocrinol 2017;233:R131–43.
[10] Lopaschuk GD. Fatty acid oxidation and its relation with insulin resistance and associated disorders. Ann Nutr Metab 2016;68(Supplement 3):15–20.
[11] Patel TP, Rawal K, Bagchi AK, Akolkar G, Bernardes N, Dias DDS, Gupta S, Singal PK. Insulin resistance: an additional risk factor in the pathogenesis of cardiovascular disease in type 2 diabetes. Heart Fail Rev 2016;21:11–23.
[12] Ingelsson E, Sundström J, Arnlöv J, Zethelius B, Lind L. Insulin resistance and risk of congestive heart failure. JAMA 2005;294:334–41.
[13] Vardeny O, Gupta DK, Claggett B, Burke S, Shah A, Loehr L, Rasmussen-Torvik L, Selvin E, Chang PP, Aguilar D, et al. Insulin resistance and incident heart failure the ARIC study (Atherosclerosis Risk in Communities). JACC Heart Fail 2013;1:531–6.
[14] Greene SJ, Fonarow GC. Insulin resistance in heart failure: widening the divide between reduced and preserved ejection fraction? Eur J Heart Fail 2015;17:991–3.
[15] Fu F, Zhao K, Li J, Xu J, Zhang Y, Liu C, Yang W, Gao C, Li J, Zhang H, et al. Direct Evidence that myocardial insulin resistance following myocardial ischemia Contributes to Post-Ischemic Heart Failure. Sci. Rep.:17927. Sci Rep 2015;5:17927.
[16] Novo G, Manno G, Russo R, Buccheri D, Dell'Oglio S, Morreale P, Evola G, Vitale G, Novo S. Impact of insulin resistance on cardiac and vascular function. Int J Cardiol 2016;221:1095–9.
[17] Ormazabal V, Nair S, Elfeky O, Aguayo C, Salomon C, Zuñiga FA. Association between insulin resistance and the development of cardiovascular disease. Cardiovasc Diabetol 2018;17:122.
[18] Salt IP, Hardie DG. AMP-activated protein kinase: an ubiquitous signaling pathway with key roles in the cardiovascular system. Circ Res 2017;120:1825–41.
[19] Qi D, Young LH. AMPK: energy sensor and survival mechanism in the ischemic heart. Trends Endocrinol Metab 2015;26:422–9.
[20] Smith BK, Steinberg GR. AMP-activated protein kinase, fatty acid metabolism, and insulin sensitivity. Curr Opin Clin Nutr Metab Care 2017;20:248–53.
[21] Kim J, Yang G, Kim Y, Kim J, Ha J. AMPK activators: mechanisms of action and physiological activities. Exp Mol Med 2016;48:e224.

[22] Cheng L, Sun X, Hu C, Jin R, Sun B, Shi Y, Cui W, Zhang Y. In vivo early intervention and the therapeutic effects of 20(s)-ginsenoside rg3 on hypertrophic scar formation. PLOS ONE 2014;9:e113640.
[23] Cheng L, Sun X, Li B, Hu C, Yang H, Zhang Y, Cui W. Electrospun ginsenoside Rg3/poly(lactic-co-glycolic acid) fibers coated with hyaluronic acid for repairing and inhibiting hypertrophic scars. J Mater Chem B 2013;1:4428–37.
[24] Smith I, Williamson EM, Putnam S, Farrimond J, Whalley BJ. Effects and mechanisms of ginseng and ginsenosides on cognition. Nutr Rev 2014;72:319–33.
[25] Li L, Ni J, Li M, Chen J, Han L, Zhu Y, Kong D, Mao J, Wang Y, Zhang B, et al. Ginsenoside Rg3 micelles mitigate doxorubicin-induced cardiotoxicity and enhance its anticancer efficacy. Drug Deliv 2017;24:1617–30.
[26] Li L, Wang Y, Guo R, Li S, Ni J, Gao S, Gao X, Mao J, Zhu Y, Wu P, et al. Ginsenoside Rg3-loaded, reactive oxygen species-responsive polymeric nanoparticles for alleviating myocardial ischemia-reperfusion injury. J Control Release 2020;317:259–72.
[27] Tavakoli R, Nemska S, Jamshidi P, Gassmann M, Frossard N. Technique of minimally invasive transverse aortic constriction in mice for induction of left ventricular hypertrophy. J Vis Exp 2017;127:56231.
[28] deAlmeida AC, van Oort RJ, Wehrens XH. Transverse aortic constriction in mice. J Vis Exp 2010;38:1729.
[29] Ni J, Zhao Y, Su J, Liu Z, Fang S, Li L, Deng J, Fan G. Toddalolactone protects lipopolysaccharide-induced sepsis and attenuates lipopolysaccharide-induced inflammatory response by modulating HMGB1-NF-κB translocation. Front Pharmacol 2020 Feb 21;11:109.
[30] Kirshenbaum LA, Singal PK. Antioxidant changes in heart hypertrophy: significance during hypoxia-reoxygenation injury. Can J Physiol Pharmacol 1992;70:1330–5.
[31] Chen JR, Wei J, Wang LY, Zhu Y, Li L, Olunga MA, Gao XM, Fan GW. Cardioprotection against ischemia/reperfusion injury by QiShenYiQi Pill® via ameliorate of multiple mitochondrial dysfunctions. Drug Des Dev Ther 2015;9:3051–66.
[32] Boutagy NE, Rogers GW, Pyne ES, Ali MM, Hulver MW, Frisard MI. Using isolated mitochondria from minimal quantities of mouse skeletal muscle for high throughput microplate respiratory measurements. J Vis Exp 2015;105:e53216.
[33] Dong Z, Zhao P, Xu M, Zhang C, Guo W, Chen H, Tian J, Wei H, Lu R, Cao T. Astragaloside IV alleviates heart failure via activating PPARα to switch glycolysis to fatty acid β-oxidation. Sci. Rep.:2691. Sci Rep 2017;7:2691.
[34] Jiang M, Ni J, Cao Y, Xing X, Wu Q, Fan G. Astragaloside IV attenuates myocardial ischemia-reperfusion injury from oxidative stress by regulating succinate, lysophospholipid metabolism, and ROS Scavenging System. Oxid Med Cell Longev 2019 Jun 24;2019:9137654.
[35] Geiger R, Rieckmann JC, Wolf T, Basso C, Feng Y, Fuhrer T, Kogadeeva M, Picotti P, Meissner F, Mann M, et al. L-arginine modulates T cell metabolism and enhances survival and anti-tumor activity. Cell 2016 Oct 20;167:829–842.e13.
[36] Fillmore N, Levasseur JL, Fukushima A, Wagg CS, Wang W, Dyck JRB, et al. Uncoupling of glycolysis from glucose oxidation accompanies the development of heart failure with preserved ejection fraction. Mol Med 2018;24:3.
[37] Gibb AA, Hill BG. Metabolic coordination of physiological and pathological cardiac remodeling. Circ Res 2018;123:107–28.
[38] Shao D, Tian R. Glucose transporters in cardiac metabolism and hypertrophy. Compr Physiol 2015;6:331–51.